

# Decreased Membrane Deformability in Melanesian Ovalocytes from Papua New Guinea

ALLAN SAUL, GRETTEL LAMONT, WILLIAM H. SAWYER,\* and CHEV KIDSON

Queensland Institute of Medical Research, Brisbane, Queensland, Australia 4006; and \*Russell Grimwade School of Biochemistry, University of Melbourne, Parkville, Victoria, Australia 3052. Dr. Lamont's present address is The Rockefeller University, New York 10021

**ABSTRACT** We examined the ability of Melanesian ovalocytes from Papua New Guinea to be deformed in order to probe the resistance of these cells to invasion by several species of malaria parasite. We found ovalocytes were refractile to drug-induced endocytosis, that they formed abnormal rouleaux, showed reduced deformability when aspirated into 0.6- $\mu\text{m}$  diameter pores in polycarbonate sieves, and failed to crenate when mounted under a glass coverslip. No substantial differences were found between normocytes and ovalocytes in their initial rate of filtration through 4.5- $\mu\text{m}$  pore polycarbonate sieves, their membrane fluidity as measured by the rate of depolarization of fluorescent probes or the rate of extraction of cytoskeletal proteins in low ionic strength buffers. We conclude that the resistance of ovalocytes to undergo localized deformation might be significant in explaining the resistance of these cells to invasion by malarial merozoites.

Ovalocytic erythrocytes from Melanesians living in parts of coastal Papua New Guinea hyperendemic for malaria are resistant to invasion by merozoites of *Plasmodium falciparum* (1, 2) and *Plasmodium knowlesi* (3) in vitro. Morphologically similar ovalocytic cells are also found at a high frequency in aboriginal populations throughout Southeast Asia in areas endemic for malaria. These cells can be distinguished from elliptocytes found at a low frequency throughout the world both by their morphology and their heat stability (1).

There is selective depression of several blood group antigens associated with hereditary ovalocytosis (4) and rouleaux formation has been reported to be absent or abnormal (5). As the invasion of erythrocytes by malarial parasites (6), and rouleaux formation (7) are all accompanied by deformation of the erythrocyte membrane, it was important to determine the deformability of ovalocyte membranes. A number of experimental techniques are available for investigating membrane deformability in erythrocytes. These include drug-induced endocytosis (8, 9), erythrocyte filterability (10, 11), and the ability of the membrane to be aspirated into small pores (12).

Endocytosis can be induced in erythrocytes by the amphipathic cations primaquine (8), vinblastine, chlorpromazine, and hydrocortisone (9). It has been postulated that this drug-induced endocytosis can occur via different pathways since the morphology of primaquine- and chlorpromazine-induced

vacuoles differs (13) and incubation condition requirements vary. Primaquine-induced endocytosis is ATP-dependent while chlorpromazine-induced endocytosis continues at low ATP levels (14).

Many models have been proposed for endocytosis. These include the suggestions that (a) primaquine increases membrane fluidity, thus enabling membrane invagination (15), that (b) expansion of the cytoplasmic phospholipid bilayer relative to the exterior layer occurs due to insertion of the amphipathic cations (16), and that (c) depletion of spectrin occurs in areas of the membrane which then form vacuoles (14). Membrane fluidity can be measured by the depolarization of light emitted from fluorophores under going rotational diffusion in the membrane (17) and has been applied to the study of the microviscosity of erythrocytes infected with the rodent malaria, *Plasmodium berghei* (18). Under conditions of low ionic strength, erythrocyte membranes can be depleted of spectrin. Erythrocyte membranes from patients with hereditary spherocytosis show reduced rates of spectrin/actin dissociation under these conditions (19); erythrocytes from these patients also show reduced drug-induced endocytosis (20).

Erythrocytes are remarkably deformable and can be forced through sieves with a pore size considerably less than the diameter of an erythrocyte. Filtration techniques using sieves with pore sizes of 3 to 5  $\mu\text{m}$ , measure both the deformability of the cells and the proportion of nondeformable cells in the

population (10, 11). The deformability of cells measured by this technique is extremely sensitive to changes in the surface to volume ratio of the cells.

Aspiration of erythrocyte membranes into sieves or glass pipettes with much smaller pore sizes (<1  $\mu\text{m}$ ) provides a different measure of deformability that is primarily dependent on intrinsic membrane properties (12). The degree to which membranes can be aspirated into such pores depends upon two properties (21). One is the resistance of the membrane to bending and can be measured by the pressure required to bend the membrane sufficiently enter the pore (21) and the other is the shear elasticity of the membrane, which can be measured by the force required to elongate the membrane surrounding the pore to extend the protrusion within the pore (21).

Here we describe differences between ovalocytes and normocytes in those properties that depend upon deformability of the membrane. Those measured were drug-induced endocytosis, aspiration into 0.6- $\mu\text{m}$  polycarbonate sieves, and rouleaux formation. Relationships between reduced membrane deformability and resistance to merozoite invasion are discussed.

## MATERIALS AND METHODS

**Blood:** Venous blood was collected into heparin or acid-citrate-dextrose from Melanesian donors known to have ovalocytes that are resistant to invasion by *P. falciparum* in vitro and from donors with sensitive normocytes. In each experiment normocytes were included as controls. The blood was stored at 4°C.

**Drug-induced Endocytosis:** The erythrocytes used in these experiments were washed twice in Krebs-Ringer-phosphate buffer (pH 7.4) supplemented with 0.2% glucose, and the buffy coat was removed. If the sample had been stored for >48 h after collection, the erythrocytes were metabolically repleted by incubation in 1 mM adenine, 10 mM inosine, 14 mM glucose in 130 mM NaCl, and 15 mM phosphate (pH 7.4) for 2 h at 37°C before treatment (9).

The extent of endocytosis was determined by three methods. (a) Internalization of  $^{57}\text{Co}$ -cyanocobalamin: when complexed with serum proteins,  $^{57}\text{Co}$ -cyanocobalamin binds to the surface of erythrocytes and is thus internalized in endocytic vacuoles. When the external complexes are removed by trypsin treatment, the increase in remaining radiolabel compared with nondrug-treated controls reflects the degree of vacuolation. The method described by Ben-Bassat et al. (9) was followed, using final concentrations of 1 mM primaquine diphosphate and 0.6 mM chlorpromazine hydrochloride. (b) Electron microscopy: a 30% suspension of cells in Krebs-Ringer-phosphate buffer was incubated with 1 mM primaquine or 0.6 mM chlorpromazine for 2 h at 37°C. The cells were washed twice in cold phosphate-buffered saline, and then fixed in 0.1 M cacodylate, 2.5% glutaraldehyde, and 0.4 M glucose (pH 7.4). The cells were washed once in 0.1 M cacodylate and postfixed in osmium tetroxide (1% in 0.1 M cacodylate) for 1 h at 4°C. After dehydration for 10 min each in 10%, 20%, 50%, 75%, 95%, and 100% ethanol, the cells were embedded in Spurr-embedding medium. Thin sections were cut with a diamond knife and examined using a Philips 400 electron microscope. (c) Phase-interference microscopy: a 1% suspension of cells was incubated with a range of primaquine concentrations for 1 h at 37°C, pelleted and fixed by replacing the supernatant with 1% glutaraldehyde in phosphate-buffered saline. Cells were mounted and the fraction of deformed or vacuolated cells counted.

**Membrane Fluidity Measurements:** Membrane fluidity was determined in washed erythrocyte ghosts by measuring the polarization of the emitted fluorescent light of a series of probes inserted in the membrane. The amount of depolarization of this light is a measure of the movement of the probe during its excited lifetime. Two types of fluorescent probes were used for the measurement of membrane fluidity; 1,6-diphenyl-1,3,5-hexatriene (17) and a set of fluorescent fatty acid probes (n-(9-anthroxlyoxy) fatty acids, n = 2, 6, 9, 12, and 16) prepared from the corresponding hydroxy fatty acids by anhydride synthesis (22). The set of fatty acid probes was used to measure the fluidity gradient through the membrane since the distance between the surface of the membrane and the fluorescent dye varies with its point of conjugation to the acyl chain of the fatty acid.

The erythrocyte ghosts were prepared from 15 ml blood that was washed with saline immediately after collection and the buffy coat removed. The cells

were lysed by the addition of ice-cold lysis buffer (6 mM sodium phosphate [pH 7.6]) to give a final volume of 50 ml and 100  $\mu\text{l}$  of 100 mM phenylmethylsulfonyl fluoride were added. The mixture was left on ice for 10 min before diluting to 400 ml with lysis buffer and centrifuging at 20,000 g for 15 min at 4°C. The supernatant was discarded. The ghosts were gently resuspended in a further 400 ml of lysis buffer, the small gelatinous pellet remaining after resuspension of the ghosts was discarded and the ghosts collected by centrifugation at 20,000 g for 15 min at 4°C. Membrane protein concentrations were measured by the dye-binding method of Bradford (23).

Fluorescence polarization was determined in duplicate at 25°C using a modification of the method described by Howard and Sawyer (18). Briefly, ghosts were resuspended at 30  $\mu\text{g}$  protein/ml in 1 mM imidazole, 6 mM KCl at pH 7.4, 1,6-diphenyl-1,3,5-hexatriene and the fatty acid probes were added to give final concentrations of 0.5 and 4  $\mu\text{M}$ , respectively. The uptake of the probes was allowed to come to equilibrium, and the polarization determined with an instrument constructed according to the design of Thulborn and Sawyer and Bashford et al. (22, 24).

**Membrane Protein Dissociation:** The time course for the dissociation of proteins, hereafter called spectrin/actin, from erythrocyte stroma was determined as described by Hill et al. (19). Briefly, a portion of the ghosts prepared for the fluidity measurements were suspended in 6 mM KCl, 1 mM imidazole, pH 7.6, then diluted fivefold into 0.1 mM EDTA at 21°C. At successive time intervals, samples were removed, centrifuged at 150,000 g for 30 s at 4°C using an air-driven ultracentrifuge (Beckman Airfuge [Beckman Instruments, Inc., Palo Alto, CA]) and the amount of released spectrin/actin determined by protein assay of the supernatant.

**Erythrocyte Filterability:** This was determined by the flow of washed erythrocytes through a 2.5-cm diameter, 4.5- $\mu\text{m}$  pore size polycarbonate membrane (Nuclepore, Pleasanton, CA) (10). The blood was washed three times in saline, the buffy coat removed, and after hemocytometer cell counts, resuspended to  $10^7$  cells/ml in saline. The time taken for successive 1- or 2-ml vol to pass through the filter at a pressure of 10 cm of  $\text{H}_2\text{O}$  was measured. The logarithm of the flow rate for each volume was plotted against the total volume that had passed through the filter. The line of best fit was calculated by linear regression analysis and the initial flow rate was determined from this line. This value, divided by the initial flow rate of saline, was used as a measure of deformability while the slope of the line (rate of flow decrement) gave an indication of the proportion of nondeformable cells present. The mean corpuscular volume of the samples used in the deformability experiments was measured using a Coulter S-Plus analyser with a 50- $\mu\text{m}$  diameter orifice.

**Membrane Deformability:** Erythrocyte membrane deformability was measured by aspirating cells into polycarbonate sieves with 0.6- $\mu\text{m}$  diameter pores (Nuclepore Corp., Pleasanton, CA) using the method of Brailsford et al. (21). Briefly, cells were aspirated into the sieve and fixed with 1% glutaraldehyde in phosphate-buffered saline under a constant hydrostatic pressure. The sieve with cells attached, was dehydrated, mounted with the cells against a coverslip, and the sieve dissolved in chloroform. The coverslips were coated with aluminium or gold and examined using a scanning electron microscope. The length of the protrusions were measured on photographs of suitably orientated cells. The bending stiffness of the membranes was calculated from the minimum pressure needed to produce protrusions with a length greater than the radius of the pores using the equation derived by Brailsford et al. (21), i.e.,

$$\text{bending stiffness} = \text{pressure} \times (\text{pore radius})^3/5.66. \quad (1)$$

The contraction ratio of the membrane at the entrance to the pores ( $\lambda_1$ ) was calculated as

$$\lambda_1 = \sqrt{2 \times (\text{length of protrusion})/(\text{pore radius})}. \quad (2)$$

The elastic modulus was also calculated using the method of Brailsford et al. (21). In this method, a linear stress-strain relationship is not assumed and the data are fitted to the equation

$$T_p = M(\lambda_1^2 - 1)^\psi/(2^\psi - 1), \quad (3)$$

where  $T_p$  is the axial tension,  $M$  is the elastic modulus, and  $\psi$  is a constant to be determined. The axial tension in the membrane at the entrance to the pore was calculated from the pressure applied, and the size of the hole (21), and corrected for pressure required to maintain the strain energy stored in the cylindrical portion of the protrusion (21). Eq. 3 can be transformed to

$$\log(\lambda_1^2 - 1) = (1/\psi)\log(T_p) - (\log(M/(2^\psi - 1)))/\psi, \quad (4)$$

which was used to calculate  $1/\lambda$  (and thereby  $\lambda$ ) and  $M$  by linear regression analysis.

**Rouleaux Formation:** Rouleaux were induced in washed erythrocytes using the method of Sewchand and Canham (7). Cells were mixed with 1%, 5%, and 10% wt/vol swine skin gelatin (Type II, Sigma Chemical Co., St. Louis, MO) in Tris-buffered saline (NaCl, 8.3 g/liter; KCl, 0/42 g/liter; CaCl<sub>2</sub>, 0.24 g/liter; NaHCO<sub>3</sub>, 0.20 g/liter; glucose 1.0 g/liter trishydroxymethylamino-methane, 37.6 g/liter, pH adjusted to 7.4 with HCl) in an inverted cell covered with a glass coverslip. Forming rouleaux were observed using an Olympus inverted microscope with 40× interference optics and were photographed for later analysis at 30-s intervals. Rouleaux were also observed in a drop of undiluted acid-citrate-dextrose-treated blood under a coverslip.

**Echinocyte Formation:** The ability of erythrocytes to form echinocytes was examined following two treatments. (a) a 5 μl drop of blood diluted with phosphate-buffered saline was placed at the edge of a 22-mm diameter coverslip resting on a microscope slide. The cells were examined immediately after the liquid had been drawn under the coverslip using the optics described above. (b) 2 μl of a 10% suspension of washed cells in saline was added to 100 μl of Tris-buffered saline adjusted to pH 7.4, 7.8, 8.2, 8.6, 9.0, or 10.0 with HCl, in the wells of a flat-bottomed, 96-well tissue culture tray. The cells were observed with an inverted phase contrast microscope using a dry 20× objective immediately, after 30 min and after 4 h at room temperature.

## RESULTS

### Drug-induced Endocytosis

Erythrocytes from two ovalocytic subjects were treated with primaquine with a sample taken from one of these subjects on two separate occasions. Results of these experiments are summarized in Table I. Significantly more <sup>57</sup>Co had been retained in treated than in untreated normocytes indicating that a substantial area of membrane had been internalized. However, there was little endocytosis in either of the primaquine-treated ovalocyte samples: in neither case was the retention of <sup>57</sup>Co significantly different from untreated controls. There was no significant difference in <sup>57</sup>Co retention following primaquine treatment of metabolically repleted and freshly collected normocytes (data not shown). Electron microscopy of primaquine-treated erythrocytes showed that there were many more vacuolated normocytes than ovalocytes, and the rare vacuolated ovalocytes had fewer vacuoles per cell. As judged by light microscopy, few ovalocytes became vacuolated over a range of primaquine concentrations (Table II). However both ovalocytes and normocytes were deformed by the drug at similar concentrations. In the 0.312- and 0.625-mM concentrations invaginations of the cell membrane and stomatocytes were seen in both ovalocytes and normocytes. At higher concentrations, the normocytes became spherocytic, while no further changes occurred in the ovalocytes, the cells remaining oval and approximately discoid at the highest concentration tested (1.25 mM).

Treatment of ovalocytes and normocytes with chlorpromazine resulted in significantly more retention of <sup>57</sup>Co in

treated than untreated normocytes while the ovalocytes did not retain significantly more <sup>57</sup>Co than the untreated controls (Table III). Electron microscopy of chlorpromazine-treated erythrocytes showed that vacuolation of ovalocytes did occur but the vacuoles in ovalocytes were considerably smaller than those in normocytes (Fig. 1).

### Rouleaux Formation

Rouleaux formation in both ovalocytic and normocytic samples was dependent upon the concentration of swine skin gelatin. Neither sample formed rouleaux in a 1% solution of gelatin, and the frequency and rate of formation was higher in the 10% than the 5% solution. While the frequency of rouleaux formation was similar for ovalocytes and normocytes in higher gelatin concentrations, the type of rouleaux formed differed markedly. Normocytes formed rouleaux predominantly by the "sliding mode" described by Sewchand and Canham (7). In this mode the cells touch, then one cell slides over the other cell until the cells are effectively coaxial. Formation of rouleaux in ovalocytes commenced with a similar sliding motion. However, instead of the contact area between the cells increasing, both cells remained biconcave, thus the contact area was limited. In many cases, the sliding ceased when the edge of one cell reached the center of the other. When this happened, rouleaux formation sometimes ceased with the cells pivoting about the line of contact to leave the pair lying at right angles. Rouleaux present in whole blood without the addition of inducing agents also showed marked differences between ovalocytes and normocytes as shown in Fig. 2. Ovalocyte rouleaux were both less regular and less densely packed. It appeared that the individual cells had retained their biconcave morphology.

TABLE I  
<sup>57</sup>Co-Cyanocobalamin Internalization after Primaquine Treatment

	Disintegrations per minute (dpm) (mean ± SD)		
	Untreated	Primaquine-treated	p*
Normocyte 1*	89.7 ± 0.9	102.0 ± 1.5	<0.002
Normocyte 2*	95.3 ± 1.2	125.3 ± 6.3	<0.001
Ovalocyte 1	92.3 ± 1.8	95.3 ± 0.9	>0.05
Ovalocyte 2	96.6 ± 2.0	99.0 ± 1.2	>0.1

\* Data shown for normocyte controls collected concurrently with ovalocytes.  
\* Determined by Student's *t* test.

TABLE II  
<sup>57</sup>Co-Cyanocobalamin Internalization after Chlorpromazine Treatment

	dpm (mean ± SD)		
	Untreated	Chlorpromazine-treated	p*
Normocyte 1*	102.7 ± 2.7	144.0 ± 6.1	<0.001
Normocyte 2*	128.3 ± 6.1	199.0 ± 8.9	<0.001
Ovalocyte 1	125.7 ± 14.6	115.0 ± 6.1	>0.1
Ovalocyte 2	120.3 ± 2.3	120.7 ± 3.1	>0.1
Ovalocyte 3	103.7 ± 3.1	104.0 ± 3.6	>0.1

\* Data shown for normocyte controls collected concurrently with ovalocytes.  
\* Determined by Student's *t* test.

TABLE III  
Concentration Dependence of Primaquine on Deformation and Vacuolation

Primaquine concentration mM	Normocytes		Ovalocytes	
	Deformed*	Vacuolated	Deformed	Vacuolated
0.000	7	0	13	0
0.312	61	22	58	1
0.625	98*	84	95	5
1.250	100*	99.5	100*	4

\* Includes vacuolated cells.

\* Predominantly biconcave and stomatocytic.

\* Predominantly spherocytes.

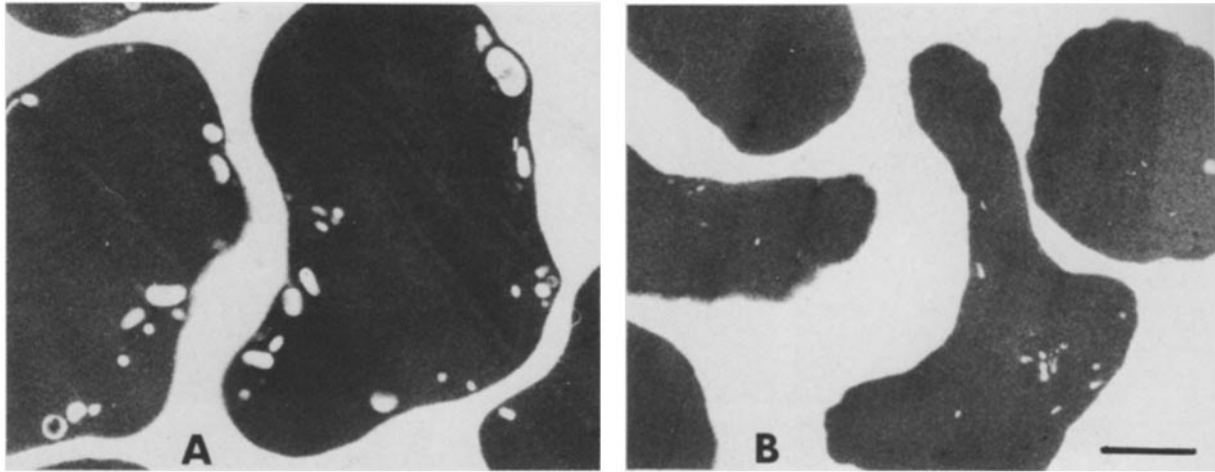


FIGURE 1 Electron micrographs of chlorpromazine treated normocytes (A) and ovalocytes (B). There were 8.21 vacuoles per normocytic cell section and 4.17 per ovalocytic cell section. The samples were stained with uranyl acetate/lead citrate after sectioning. Bar, 1  $\mu\text{m}$ .  $\times 12,500$ .

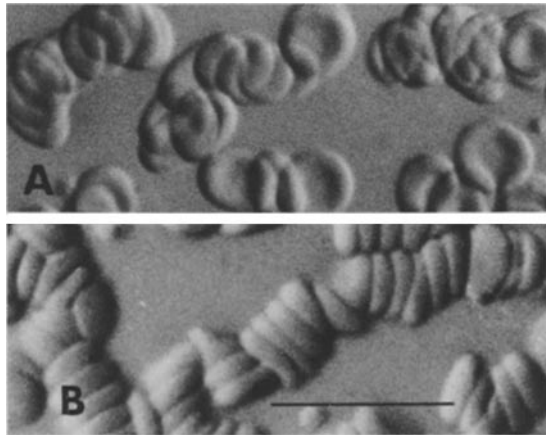


FIGURE 2 Rouleaux present in ovalocytic blood (A) and normocytic blood (B). Bar, 20  $\mu\text{m}$ .  $\times 1,250$ .

### Echinocyte Formation

When diluted normocytic blood was drawn under a coverslip, all cells invariably formed echinocytes. This was independent of the dilution over a 1:1 to 1:100 range. This is in marked contrast to the behavior of ovalocyte samples where no cells crenated (Fig. 3). When subjected to the same treatment, the cells present in both normocytic or ovalocytic undiluted blood did not crenate, but were all present as rouleaux. Although glass that was cleaned in either alcoholic KOH or chromic acid was able to induce echinocytes from normocytes, this transition was abolished by pretreating the glass surfaces with 1 mg/ml bovine serum albumin in phosphate-buffered saline for 10 min at room temperature and then blotting them dry. There was a marked difference in the ability of alkaline pH to induce echinocytes. Normocytes all became echinocytic at pH 8.2 and higher in the time taken to mix the samples. Ovalocytes did not become echinocytic at any pH tested.

### Erythrocyte Filterability and Volume

The mean initial flow rate for two ovalocyte samples compared with saline ( $0.684 \pm 0.231$  ml/s) was not significantly

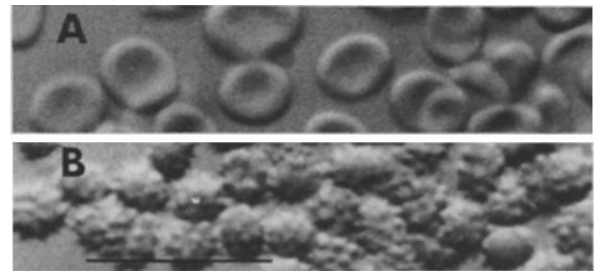


FIGURE 3 Morphology of ovalocytes (A) and normocytes (B) after a 10% dilution of blood in PBS was drawn under a coverslip. Bar, 20  $\mu\text{m}$ .  $\times 1,250$ .

different ( $P > 0.05$ ) to the mean initial flow rate for three normocyte samples ( $0.437 \pm 0.146$  ml/s). Thus ovalocytes are able to pass through a filter at least as easily as normocytes, if not more so. However, the mean rate of flow decrement of the ovalocytes ( $0.023 \pm 0.020$ ) was significantly less ( $P < 0.01$ ) than that for the normocytes ( $0.065 \pm 0.023$ ), indicating that more nondeformable cells were present in the normocyte than the ovalocyte samples. The reason for this difference was not established. It may have been due to the presence of a small proportion of echinocytic cells in the normocytes samples that were totally absent from the ovalocyte samples. The mean corpuscular volumes of the two ovalocytic samples used in the filterability experiments were 74.0 fl and 80.5 fl while those of the three normocytic samples were 86.6, 89.5, and 83.8 fl.

### Aspiration into Polycarbonate Sieves

The behavior of normocytes when aspirated into the 0.6- $\mu\text{m}$  pores was similar to the results published by Brailsford et al. (21): membrane enters the pores at a hydrostatic pressure of  $< 8$  mm. However, an hydrostatic pressure between 24 and 32 mm was required before membranes of any cells in the ovalocyte sample entered the pores (Fig. 4). From these data, the bending stiffness of normocytes is  $\sim 3 \times 10^{-12}$  dynes/cm and that of ovalocytes is  $1.3 \times 10^{-11}$  dynes/cm. The value for normocytes closely agrees with the value published by Brailsford et al. (21).

The compression ratio of membrane surrounding the pore

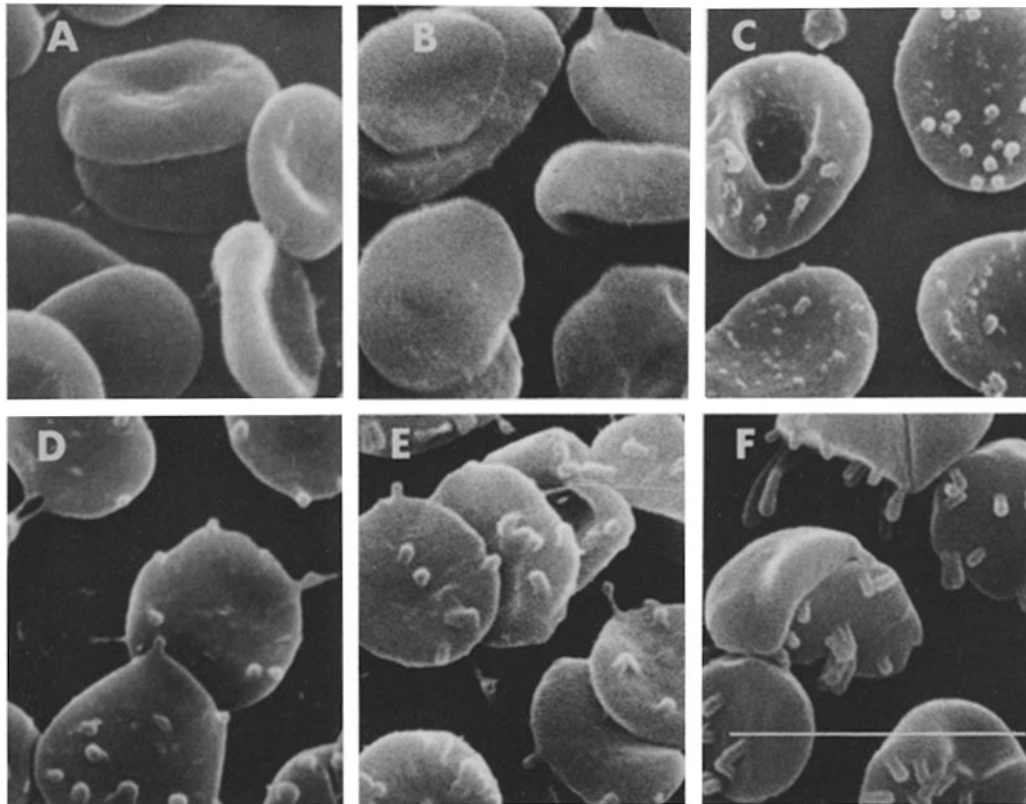


FIGURE 4 Appearance of the protrusions on ovalocytes (A–C) and normocytes (D–F) after aspiration into polycarbonate membranes. A hydrostatic pressure of 8, 16, and 32 mm of water was applied to samples A and D, B and E, and C and F, respectively. Bar, 10  $\mu\text{m}$ .  $\times 4,000$ .

is shown in Table IV at a series of pressures for both normocytes and ovalocytes. The value  $1/\psi$  was calculated from these data for both normocytes and ovalocytes using a linear regression analysis based upon equation (4). For comparison, the data of Brailsford et al. (21) for normocytes was also analysed. The value for ovalocyte membranes was 1.0, thus suggesting that over the range of pressures used, ovalocyte membranes have a linear stress-strain relationship. However, the value for normocytes in this experiment was 0.53. This value was significantly different from 1.0 ( $P < 0.001$ ) but was not significantly different from the value of 0.36 ( $P > 0.1$ ) calculated for the data of Brailsford et al. (21). Thus, as was found by these workers, the stress strain relationship for normocyte membranes is far from linear. The values of the elastic shear modulus for ovalocyte and normocyte membranes calculated using the experimentally determined values of  $\lambda$  are  $1.0 \times 10^{-2}$  dynes/cm and  $2.0 \times 10^{-3}$  dynes/cm, respectively. The corresponding value for the data of Brailsford et al., is  $1.2 \times 10^{-3}$  dynes/cm when using the full range of their data and  $1.7 \times 10^{-3}$  when their data is restricted to the range covered by our measurements.

#### Membrane Microviscosity

The polarization measured at 25°C with the 1,6-diphenyl-1,3,5-hexatriene probe was  $0.280 \pm 0.006$  and  $0.297 \pm 0.007$  for the normocytic and ovalocytic membranes, respectively. These values correspond to viscosities of  $3.52 \pm 0.20$  and  $4.13 \pm 0.32$  poise, based on a lifetime of 10 ns. The results obtained with the fatty acid probes showed no significant difference between normocyte and ovalocyte at any transverse position in the bilayer leaflet.

TABLE IV  
Aspiration of Membranes into Pores

Cell type	Water pressure cm	Sample size	$\lambda_1$ (+ SE)	$T_p$ dynes/cm	Corr $T_p^*$ dynes/cm
Normocytes	0.6	—	<1.0	0.00088	
Normocytes	0.8	32	2.30 (0.03)	0.00118	0.00110
Normocytes	1.6	40	2.60 (0.05)	0.00235	0.00231
Normocytes	3.2	25	3.20 (0.04)	0.00470	0.00466
Ovalocytes	2.4	—	<1.0	0.00353	
Ovalocytes	3.2	11	2.34 (0.04)	0.00470	0.00452
Ovalocytes	4.0	13	2.60 (0.03)	0.00588	0.00570
Ovalocytes	5.6	24	3.00 (0.04)	0.00823	0.00805

\* Corrected for bending stiffness.

#### Spectrin Extractibility

No difference was observed between the amount of spectrin extracted from normocytic or ovalocytic ghosts. These results are consistent with earlier findings (1) that the amount of spectrin is similar in both normocytes and ovalocytes. Under the conditions used, the dissociation rates of spectrin from normocytes and ovalocytes were similar and agreed with previously published results for normocytes (19).

#### DISCUSSION

As determined by the pressures required to aspirate ovalocyte or normocyte membranes into 0.6- $\mu\text{m}$  pores, ovalocyte mem-

branes have approximately four times the bending stiffness of normocyte membranes. Inspection of the raw extension data (Table IV) indicates that a higher pressure is required to obtain a given compression ratio of the membrane. This difference is still apparent after the axial tension has been corrected for the increased membrane stiffness. This suggests that the elastic shear modulus is qualitatively greater for ovalocyte membranes than for normocyte membranes. A quantitative estimate of this difference is difficult to make since the two types of membranes appear to obey different stress-strain relationships. A consequence of this different relationship is that the difference between normocytes and ovalocytes becomes greater at lower stresses. These observations have important implications for our understanding of the structure and function of the erythrocyte membrane, since the underlying molecular difference has simultaneously altered the bending stiffness, the elastic shear modulus and the form of the stress-strain relationship.

Unlike deformation measurements using micropipettes, this technique allowed enough cells to be examined to define the heterogeneity within the population. In this case, all cells in the ovalocyte sample behaved similarly including the small number of cells (~10%) that had normal morphology.

The bending stiffness of the membrane is thought to be the major factor in determining the erythrocyte shape (21, 25). As such it is not surprising that the ability of ovalocytes to form echinocytes, rouleaux, and drug-induced vacuoles should be reduced since all these processes involve bending of the membrane. Such localized deformations may also be accompanied by shear deformation and the decreased elasticity of the membrane may also play a role in the reduced response. The mechanism underlying the crenation of normocytes when placed between a coverslip and a glass slide is not known, but presumably involves membrane bending. It appears that contact between the cells and clean glass surfaces since coating the glass with albumin abolishes the activity. In addition to its value as a further example of the rigidity of the ovalocyte membrane, this observation has an important practical value. This response is currently being used as a simple method of detecting ovalocytosis in epidemiological studies designed to measure the impact of ovalocytosis on malarial infection rates.

As rouleaux formation involves both membrane deformation and cell-cell interactions (7), it is not possible to assign their abnormal formation in ovalocytes entirely to a membrane defect. However, as initiation of rouleaux formation occurs with similar frequencies and at similar concentrations of inducing agent, the evidence suggests that the inability to form tightly packed rouleaux may be a membrane-associated effect.

Primaquine induced endocytosis was also reduced as judged by <sup>57</sup>Co-cyanocobalamin internalization, electron and light microscopy. Since both the ovalocytes and normocytes began to deform at the same primaquine concentrations, it is unlikely that the observed difference was due to a different affinity of the drug for the different cell types.

It has been suggested that primaquine increases the fluidity of erythrocyte membranes before endocytosis (15). However, the results obtained with the 1,6-diphenyl-1,3,5-hexatriene probe show there are no marked differences between the microviscosity of membranes of normocytic and ovalocytic cells. The results obtained with the fatty acid probes confirm this finding and demonstrate that similar microviscosities

exist at a number of transverse positions from the surface to the center of the bilayer leaflet. The characteristic fluidity gradient across the membrane leaflet is clearly evident (26). These data exclude a preexisting difference in microviscosity as a cause of reduced endocytosis in ovalocytes.

The ability of primaquine to form invaginations as observed by light microscopy, but not vacuoles, is consistent with the increased rigidity of these cells. The energy required to bend a membrane increases as the radius of curvature of a deformation is reduced (21). As the closure of an invagination to form a vacuole requires considerable curvature at the lip of the invagination, the inability of primaquine to form vacuoles in ovalocytes may be related to the increased stiffness of the membrane at this critical step.

Vacuolation of ovalocytes was induced by chlorpromazine but ovalocyte vacuoles were considerably smaller than normocyte vacuoles. Since the amount of radiolabel incorporated is dependent on the area of external erythrocyte membrane that is internalized and not the number of vacuoles, the amount of <sup>57</sup>Co internalization reflects the size of ovalocyte vacuoles in that it is not significantly higher than the untreated controls. Since the energy involved in bending the membrane into a vacuole depends on the area involved as well as the radius of curvature, the small area of membrane internalized may again reflect the increased bending resistance of these cells. Alternatively, chlorpromazine may modify areas of the membrane as has been postulated for the formation of vacuoles in white ghosts. Vacuole formation in white ghosts that, like chlorpromazine, induce vacuolation does not require the presence of ATP and takes place in areas of membranes that become substantially spectrin-free (14). Thus an altered cytoskeleton could lead to reduced endocytosis. This may be the explanation for the decreased drug-induced endocytosis in erythrocytes from individuals with hereditary spherocytosis, where a decrease in the rate of dissociation of spectrin/actin from the remainder of the cytoskeleton has been demonstrated (19).

Cytoskeletal abnormalities would be an attractive explanation for the decreased membrane deformability, crenation, and endocytosis in ovalocytes, and would be consistent with a proposed role of the cytoskeleton in modulating thermal sensitivity (27). However, we have been unable to detect any alteration in the interaction between spectrin/actin and the rest of the cytoskeleton as measured by its ability to dissociate in low ionic strength buffers.

The altered properties of the ovalocyte membrane are in marked contrast to the ability of the whole cell to deform. As may be expected from the lack of hematological abnormalities in individuals with ovalocytosis (4), the filterability of these cells was essentially normal. In fact the marginally increased filterability may reflect a slightly smaller size or possibly be an indication of an increased surface to volume ratio for these cells. Further experiments involving more ovalocyte samples would be required to definitively answer this question.

While invasion of an erythrocyte by a malarial merozoite involves an endocytosis-like process, the observation that ovalocytes show reduced drug-induced endocytosis does not provide, by itself, a good model to explain the resistance of these cells to invasion by malaria for two reasons. First, hereditary spherocytes that also have reduced drug-induced endocytosis are susceptible to invasion by malaria (28) and, second, the evidence suggests that it is the initial binding of merozoites that is reduced, as the presence of ovalocytes failed

to effect the invasion of normocytes by merozoites and cytochalasin B failed to trap the invasion of ovalocytes by *Plasmodium knowlesi* merozoites (3).

Reduced invasion of ovalocytes is more likely to be related directly to the decreased membrane deformability. Under certain conditions, malaria merozoites will invade resealed erythrocyte ghosts. Inclusion of antispectrin antibodies inside the ghosts leads to an increased rigidity of the membrane (29) and similarly to ovalocytes, these resealed ghosts show a reduced invadability (30). Contrary to earlier reports, the membrane of hereditary spherocytes has been found to have a normal deformability (31) and this is in keeping with their normal invadability.

Since the blockage in the invasion of ovalocytes by normocytes occurs early in the invasion pathway, it is possible that the initial recognition of a erythrocyte by a parasite involves some deformation of the erythrocyte membrane. Such a deformation may be required to allow a sufficient area of the two surfaces to come together to form the initial parasite-erythrocyte complex. The marked depression of certain blood groups on ovalocytes as measured by agglutination may have a similar explanation.

We would like to thank Leanne Ingram and John Hill for technical assistance, Drs. D. Allan and C. Bishop for the scanning electron microscopy, and Dr I. Bunce and the Royal Brisbane Hospital Pathology Department for the cell sizing.

This work was supported by the National Health and Medical Research Council of Australia and by the UNDP/World Bank/World Health Organization Special Program for Research and Training in Tropical Disease.

Received for publication 8 April 1983, and in revised form 15 December 1983.

## REFERENCES

- Kidson, C., G. Lamont, A. Saul, and G. Nurse. 1981. Ovalocytic erythrocytes from Melanesians are resistant to invasion by malaria parasites in culture. *Proc. Natl. Acad. Sci. USA.* 78:5829-5832.
- Castelino, D., A. Saul, P. Myler, C. Kidson, H. Thomas, and R. Cooke. 1981. Ovalocytosis in Papua New Guinea—dominantly inherited resistance to malaria. *Southeast Asian J. Trop. Med. Public Health.* 12:549-555.
- Hadley, T., L. H. Miller, A. Saul, G. Lamont, and C. Kidson. 1982. Resistance of Melanesian elliptocytes (ovalocytes) to invasion by *Plasmodium knowlesi* and *Plasmodium falciparum* malaria parasites *in vitro*. *J. Clin. Invest.* 71:780-782.
- Booth, P. B., S. Serjeantson, D. G. Woodfield, and D. Amato. 1977. Selective depression of blood group antigens associated with hereditary ovalocytosis among Melanesians. *Vox. Sang.* 32:99-110.
- Holt, M., P. F. Hogan, and G. T. Nurse. 1981. The ovalocyte polymorphism on the Western border of Papua New Guinea. *Human Biology.* 53:23-34.
- Aikawa, M., L. H. Miller, J. Johnson, and J. Rabbege. 1978. Erythrocyte entry by malaria parasites. *J. Cell Biol.* 77:72-82.
- Sewchand, L. S., and P. B. Canham. 1978. Modes of rouleaux formation of human red blood cells in polyvinylpyrrolidone and dextran solutions. *Can. J. Physiol. Pharmacol.* 57:1213-1222.
- Ginn, F. L., P. Hochstein, and B. F. Trump. 1968. Membrane alterations in hemolysis. Internalization of plasmalemma induced by primaquine. *Science (Wash. DC).* 164:843-845.
- Ben-Bassat, I., K. G. Bensch, and S. L. Schrier. 1972. Drug-induced erythrocyte membrane internalization. *J. Clin. Invest.* 51:1833-1844.
- Gregersen, M. I., C. A. Bryant, W. E. Hammerle, S. Usami, and S. Chien. 1967. Flow characteristics of human erythrocytes through polycarbonate sieves. *Science (Wash. DC).* 157:825-827.
- Leblond, P. F., and L. Coulombe. 1979. The measurement of erythrocyte deformability using micropore membranes. A sensitive technique with clinical applications. *J. Lab. Clin. Med.* 94:133-143.
- Mohandas, N., M. R. Clark, M. S. Jacobs, and S. B. Shohet. 1980. Analysis of factors regulating erythrocyte deformability. *J. Clin. Invest.* 66:563-573.
- Greenwalt, T. J., F. U. Lau, E. M. Swierk, and R. E. Williams. 1978. Studies of erythrocyte membrane loss produced by amphipathic drugs and *in vitro* storage. *Br. J. Haematol.* 39:551-557.
- Schrier, S. L., B. Hardy, and K. G. Bensch. 1979. Endocytosis in erythrocytes and their ghosts. *Prog. Clin. Biol. Res.* 30:437-444.
- Penniston, J. T., L. Vaughan, and M. Nakamura. 1979. Endocytosis in erythrocytes and ghosts: occurrence at 0°C after ATP preincubation. *Arch. Biochem. Biophys.* 198:339-348.
- Sheetz, M. P., and S. J. Singer. 1974. Biological membranes as bilayer couples. A molecular mechanism of drug-erythrocyte interactions. *Proc. Natl. Acad. Sci. USA.* 71:4457-4461.
- Shinitzky, M., and Y. Borenholz. 1978. Fluidity parameters of lipid regions determined by fluorescence polarization. *Biochim. Biophys. Acta* 515:367-394.
- Howard, R. J., and W. H. Sawyer. 1980. Changes in the membrane microviscosity of mouse red blood cells infected with *Plasmodium berghei* detected using n-(9-anthroyloxy) fatty acid fluorescent probes. *Parasitology.* 80:331-342.
- Hill, J. S., W. H. Sawyer, G. J. Howlett, and S. S. Wiley. 1981. Hereditary spherocytosis of man. *Biochem. J.* 201:259-266.
- Schrier, S. L., I. Ben-Bassat, K. Bensch, M. Seeger, and I. Junga. 1974. Erythrocyte membrane vacuole formation in hereditary spherocytosis. *Br. J. Haematol.* 26:59-69.
- Brailsford, J. D., R. A. Korpman, and B. S. Bull. 1977. The aspiration of red cell membrane into small holes: new data. *Blood Cells.* 3:25-38.
- Thulborn, K. R., and W. H. Sawyer. 1978. Properties and locations of a set of fluorescent probes sensitive to the fluidity gradient of the lipid bilayer. *Biochim. Biophys. Acta.* 511:125-140.
- Bradford, M. 1976. A rapid and sensitive method for quantitation of microgram quantities of proteins utilizing the principle of protein-dye binding. *Anal. Biochem.* 72:248-254.
- Bashford, C. L., C. E. Morgan, and G. K. Radda. 1976. Measurement and interpretation of fluorescent polarisations in phospholipid dispersions. *Biochim. Biophys. Acta.* 426:157-172.
- Schmid-Schonbein, H., and P. Gaetgens. 1981. What is red cell deformity? *Scan. J. Clin. Lab. Invest.* 41(Suppl): 156:13-26.
- Thulborn, K. R., L. M. Tilley, W. H. Sawyer, and F. E. Treloar. 1979. The use of n-(9-anthroyloxy) fatty acids to determine fluidity and polarity gradients in lipid bilayers. *Biochim. Biophys. Acta.* 558:166-178.
- Lux, S. E., and L. C. Wolfe. 1980. Inherited disorders of the red cell membrane skeleton. *Pediatr. Clin. North Am.* 27:463-484.
- Koeweiden, E., T. Ponnudurai, and J. H. E. T. Meuwissen. 1979. *In vitro* observations on hereditary spherocytosis and malaria. *Trans. R. Soc. Trop. Med. Hyg.* 73:589-590.
- Nakashima, K., and E. Beutler. 1978. Effect of anti-spectrin antibody and ATP on deformability of resealed erythrocyte membranes. *Proc. Natl. Acad. Sci. USA.* 75:3823-3825.
- Olsen, J. A., and A. Kilejian. 1982. Involvement of spectrin and ATP in infection of resealed erythrocyte ghosts by the human malarial parasite, *Plasmodium falciparum*. *J. Cell Biol.* 95:757-762.
- Nakashima, K., and E. Beutler. 1979. Erythrocyte cellular and membrane deformability in hereditary spherocytosis. *Blood.* 53:481-485.